

Young lunar volcanic features: Thermophysical properties and formation



C.M. Elder^{a,*}, P.O. Hayne^a, J.L. Bandfield^b, R.R. Ghent^{c,d}, J.-P. Williams^e, K.L. Donaldson Hanna^f, D.A. Paige^e

^aJet Propulsion Laboratory, California Institute of Technology, Pasadena, CA 91109, United States

^bSpace Science Institute, Boulder, CO 80301, United States

^cDept of Earth Sciences, University of Toronto, Toronto, ON M5S 3B1, Canada

^dPlanetary Science Institute, Tucson, AZ 85719, United States

^eDepartment of Earth, Planetary, and Space Sciences, University of California, Los Angeles, Los Angeles, CA 90095, United States

^fAtmospheric, Oceanic and Planetary Physics, University of Oxford, Clarendon Laboratory, Oxford, UK

ARTICLE INFO

Article history:

Received 22 November 2016

Accepted 8 March 2017

Available online 9 March 2017

Keywords:

Moon

Volcanism

Infrared observations

Thermal histories

ABSTRACT

Irregular mare patches (IMPs) are small volcanic features on the lunar nearside with young model ages. Several formation mechanisms have been proposed including: caldera collapse, explosive outgassing, lava flow inflation, pyroclastic eruption, and regolith drainage. We present new observations of the four largest IMPs (Sosigenes, Ina, Cauchy-5, and Maskelyne) using the Lunar Reconnaissance Orbiter (LRO) Diviner Lunar Radiometer (Diviner) and evaluate the formation hypotheses in the context of both previous results and the results presented here. We find that the IMPs have a rock abundance slightly higher than their surrounding terrain. Comparison of the Diviner data with thermal models excludes the possibility of extensive competent rocks within ~15 cm of the surface at the IMPs. We also derive the thermal inertia at the four largest IMPs. Three appear to have thermal inertias slightly higher than typical regolith due to alteration by nearby craters or mass wasting from surrounding steep slopes, but Ina has a thermal inertia lower than the surrounding terrain. In particular, the largest smooth mound in Ina is the area with the lowest thermal inertia, suggesting that the material on the mound is less consolidated than typical regolith and/or contains fewer small rocks (<1 m). Formation by lava flows or regolith drainage is not expected to result in material with a lower thermal inertia than pre-existing regolith, so some other process such as explosive outgassing or pyroclastic eruptions must have occurred.

© 2017 Elsevier Inc. All rights reserved.

1. Introduction

Irregular mare patches (IMPs) are hypothesized lunar volcanic features (e.g. El-Baz, 1973; Garry et al., 2012; Braden et al., 2014) characterized by uneven terrain interspersed by topographically higher smooth mounds (Fig. 1). Some mounds are surrounded by the lower uneven terrain, and other mounds connect seamlessly to surrounding terrain. The first observed IMP, Ina, was discovered during Apollo 15 (Whitaker, 1972). Several other IMPs were discovered using Apollo data (e.g. Schultz, 1976; Masursky et al., 1978), but the Lunar Reconnaissance Orbiter Camera (LROC) enabled the discovery of many more features that share characteristics with Ina (e.g. Stooke, 2012; Braden et al., 2014). The list of IMPs presented by Braden et al. (2014) totals 70 IMPs whose maximum dimensions

range from 100–5000 m. Before LROC, only two craters larger than 30 m were identified within Ina. If subdued, rimless depressions were also counted as craters, crater statistics suggested a maximum age of 10 Myr for Ina (Schultz et al., 2006). Crater counting using LROC data (enabling the inclusion of smaller craters) suggests that IMPs are younger than 100 Myr (Braden et al., 2014) with crater size-frequency distributions yielding model ages of 18 Myr for Sosigenes, 33 Myr for Ina, and 58 Myr for Cauchy-5. Photometric properties, spectral properties, topographic relief, and surface texture also indicate a young age for Ina (Schultz, 1991; Schultz et al., 2000, 2006).

Typical thermal evolution models for the Moon predict that it should not have been volcanically active as recently as the IMP model ages imply, because as the mantle cools, the area capable of partially melting becomes increasingly small and deep (e.g. Taylor, 1982; Spohn et al., 2001; Ziethe et al., 2009). As the Moon cools, it also enters a state of net contraction causing global compression in the lithosphere, which hinders dike formation, propaga-

* Corresponding author.

E-mail address: catherine.elder@jpl.nasa.gov (C.M. Elder).

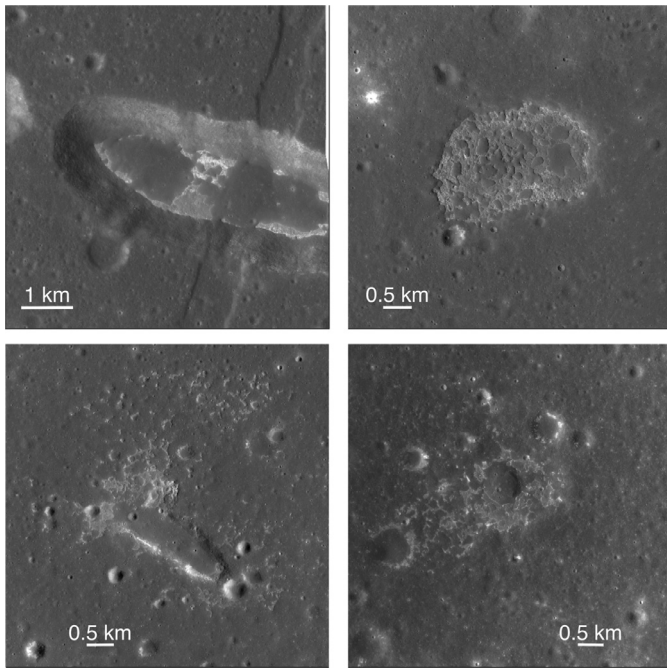


Fig. 1. LROC Narrow Angle Camera (NAC) images of a) Sosisgenes (LROC NAC M177514916; 0.5 m/pix), b) Ina (NAC mosaic: NAC_ROL_INADCALDLOA; 0.95 m/pix), c) Cauchy-5 (M1108025067; 1.2 m/pix), and d) Maskelyne (M1129269012; 1.0 m/pix). Images: NASA/GSFC/Arizona State University.

tion, and eruption (Solomon and Head, 1980). With the exception of IMPs, estimated ages of lunar volcanism support these thermal models. Apollo samples of the lunar maria range in age from approximately 3.1 to 3.9 billion years old (e.g. Nyquist et al., 1977; Papanastassiou et al., 1977). Recent measurements of a lunar meteorite suggest that magmatism continued until at least 2.9 Gyr (Fernandes et al., 2003; Borg et al., 2004). Crater size–frequency model ages of the maria suggest that lunar volcanism occurred from 4.0 to 1.2 Gyr ago with the majority occurring between 3.8 and 3.3 Gyr ago (Hiesinger et al., 2011). More recently than 3.3 Ga, there is a steep decline in volcanic activity. The most recent basalts are associated with the Procellarum KREEP Terrane (PKT), which contains an enhanced concentration of heat producing elements (Hiesinger et al., 2011). If the young model ages of the IMPs are correct and they are volcanic in origin, then they imply an approximately 1 billion year gap in volcanic activity between the youngest mare basalts and the formation of the IMPs. Thus, the young model ages of the IMPs are an anomaly compared to thermal evolution models of the Moon, radioisotope ages of Apollo samples and lunar meteorites, and model ages of basaltic flows in the maria. Therefore, understanding how the IMPs formed has important implications for understanding the thermal evolution and volcanic history of the Moon.

Several formation hypotheses have been proposed for IMPs, including: caldera collapse (El-Baz, 1973), explosive outgassing (Schultz et al., 2006), lava flow inflation (Garry et al., 2012), pyroclastic eruption (Carter et al., 2013), and regolith drainage (Qiao et al., 2016). Previous work has focused on geomorphology using images, material properties from radar data, and composition using spectroscopy. Despite a consensus on the role of volcanism in some form, the mechanism of IMP formation is still debated. Although it is possible that not all IMPs formed through the same mechanism, most previously suggested hypotheses have included arguments specific to Ina (El-Baz, 1973; Schultz et al., 2006; Garry et al., 2012; Qiao et al., 2016), so the debate cannot be resolved by arguing that IMPs do not share a formation mechanism.

In this study, we use thermal infrared data to investigate thermophysical properties of the IMPs, including rock abundance and regolith properties. These data provide a unique perspective on these intriguing features and new constraints on their geologic history. We consider only the four largest IMPs, which are covered by multiple Diviner pixels: Sosisgenes (8.335°N, 19.071°E), Ina (18.650°N, 5.300°E), Cauchy-5 (7.169°N, 37.592°E), and Maskelyne (4.330°N, 33.750°E). In the following sections, we first place the present study in the context of previous work on the IMPs. After detailing our methods, we present results and evaluate the proposed formation mechanisms with the added thermophysical constraints.

2. Background

High resolution imaging from LROC enables observations of crater morphology and crater counting of small craters (down to the meter-scale). Qiao et al. (2016) found that craters ranging in size from ~45 to 155 m in diameter on the smooth mounds of Sosisgenes show normal bowl-shaped topographic profiles and do not contain exposed boulders on crater walls. This suggests that the craters are either ancient and heavily degraded or did not penetrate the layer of fine-grained material covering bedrock (e.g. McKay et al., 1991; Cintala and McBride, 1995; Bandfield et al., 2011; Qiao et al., 2016). In contrast, small craters (~20–35 m in diameter) on Sosisgenes' lower uneven units do excavate boulders, which suggests that bedrock is within 1.5–2.5 m of the surface (Qiao et al., 2016). Phase ratio images, which are the ratio of two images taken at different phase angles, can reveal the sub-resolution texture of the regolith by removing the inherent albedo variations of the scene (Kaydash et al., 2011). At eastern Sosisgenes and eastern Ina, phase ratio images show that the smooth mounds have “slightly smoother sub-resolution surface texture[s]” than typical mature lunar regolith, and the lower uneven unit has “significantly lower sub-resolution roughness” than typical lunar mature regolith (Qiao et al., 2016).

In addition to their unusual morphology, IMPs have spectral properties that are unique from their surrounding terrain. These different spectral properties were first observed by Apollo 17 astronauts who noted that although the raised bumps (mounds) are the same color as the surrounding material, the floor material in Ina is a light bluish gray relative to the surrounding terrain (Evans and El-Baz, 1973). Schultz et al. (2006) investigated the spectral properties of Ina using data from Clementine and found that the overall spectral properties of the bright materials within Ina are most similar to fresh mare craters in Tranquillitatis. Clementine color ratio images confirm that Ina is bluer (higher 415 nm/750 nm ratio) than its surroundings. This indicates the presence of more mafic materials and is consistent with high-titanium mare basalts (Schultz et al., 2006). The bright, rubbly materials within Ina exhibit the strongest mafic ratios. The interior of Ina also has a strong 750 nm/950 nm ratio which indicates less weathered and/or more mafic materials (Schultz et al., 2006). A more recent investigation using higher spectral and spatial resolution Moon Mineralogy Mapper (M^3) data revealed that the ferrous absorption associated with relatively unweathered materials is related to the uneven terrain (Staid et al., 2011). Staid et al. (2011)'s results also confirm previous studies that showed the materials within Ina resemble freshly exposed high-titanium basalts exposed in craters in Mare Tranquillitatis. Also using M^3 data, Grice et al. (2016) showed that the smooth deposits in Sosisgenes are less optically mature than the surrounding mare, and the uneven deposits are less optically mature than both the surrounding mare and the smooth deposits. The spectral signatures of the uneven and smooth deposits in Sosisgenes are similar in composition to the surrounding mare. However, data from Diviner shows a compositional difference between the un-

even and smooth deposits in Sosigenes (Donaldson Hanna et al., 2016).

Radar observations have been used to study the surface and shallow subsurface of several IMPs (Carter et al., 2013). Radar observations at Ina show an enhanced circular polarization ratio (CPR) from the edges of the depression and from the interior uneven terrain (Carter et al., 2013). CPR values surrounding the depression are similar to the surrounding crater plains (Carter et al., 2013). The Cauchy-5 IMP, located on top of a dome, is surrounded by a low albedo and low CPR region (Carter et al., 2013). This suggests that the upper centimeters to meters of the Cauchy-5 dome are fine-grained, block-poor material (Carter et al., 2013). Hyginus crater, which also features an IMP, is also surrounded by low-albedo, low CPR terrain. The inside of the crater has slightly elevated CPR values relative to the surrounding terrain (Carter et al., 2013). These different CPR properties at different IMPs imply that the near surface structure is not the same at all IMPs.

2.1. Formation hypotheses

IMPs have confounded the lunar community since the discovery of Ina during Apollo 15 (El-Baz, 1973). Since then, the discovery of more IMPs and the availability of spectral data, radar observations, and higher resolution visible imagery have all led to new hypotheses explaining how the IMPs might have formed. However, despite this additional data, there is still significant debate about the formation of IMPs (e.g. Garry et al., 2012; Head and Wilson, 2016). In this section, we summarize the leading hypotheses for IMP formation.

2.1.1. Caldera collapse

Based on Apollo 15 and 17 images that show Ina (then called “D-Caldera”) is a 300 m deep depression at the top of an 18-km wide dome, El-Baz (1973) suggested that Ina is a collapsed caldera on top of an extrusive volcanic dome. They argued that the surface of the dome is smoother and has fewer craters per unit area than the surrounding terrain and thus post-dates the surrounding mare basalt. El-Baz (1973) suggest that the center of the dome collapsed to form Ina, and that pre-existing faults in the mare unit may have caused it to be non-circular. In this scenario, small volcanic extrusions after the collapse would have formed the smooth mounds on the floor of Ina (El-Baz, 1973; Strain and El-Baz, 1980).

2.1.2. Explosive outgassing

Schultz et al. (2006) suggested that Ina and the other IMPs that had been identified at the time could have formed by sudden degassing removing the thick regolith surface layer to expose a long-buried high-titanium basalt surface. In this scenario, although the original basaltic surfaces comprising the lower uneven unit in Ina are at least 3.5 Gyr old, they are freshly exposed by the removal of material by outgassing. The faint halo and raised rim encircling Ina would have been formed by regolith ejected during a relatively low energy process with limited ballistic range. Schultz et al. (2006) also suggested that the outgassing volatiles might include CO₂, H₂O, or radon.

2.1.3. Lava flow inflation

Garry et al. (2012) used LROC images and a Digital Terrain Model (DTM) to compare the morphology of Ina to terrestrial inflated lava flows. They found that the morphology and dimensions of the high and low units are similar to those of flows in Hawai'i, New Mexico, and Idaho. They suggested that the mounds in Ina are examples of inflation, and the lower uneven terrain formed by breakouts from the inflating mounds. Garry et al. (2012) argued that mass wasting exposed fresh surfaces in the blocky units of Ina. However, they also identified some differences between Ina

and the terrestrial analogs they studied. The main differences are Ina formed within a depression, no vent source is observed, and no cracks or lava-rise pits are observed on the mounds. They argued that because the top of the mounds of Ina are more curved than the steep margins of terrestrial inflated sheet lobes, cracks could be narrower (and thus harder to observe remotely) than on Earth or that the cracks have simply degraded over time (Garry et al., 2012).

2.1.4. Pyroclastic eruptions

Different IMPs exhibit different radar backscatter properties, which implies that they have different near-surface properties. At some IMPs Carter et al. (2013) measured CPR values similar to those measured at known pyroclastic deposits. For example, Cauchy-5 is surrounded by a region with low CPR, which suggests material that is fine-grained and block poor, possibly a pyroclastic deposit containing few rock fragments compared to regolith (Carter et al., 2013). The CPR values in the terrain surrounding Hyginus are similar to those measured at the nearby Vaporum pyroclastic deposit (Carter et al., 2009, 2013) suggesting a similar origin. The interior of Hyginus has a slightly higher CPR value than the surrounding pyroclastics which could be due to the rough hills seen inside the crater or could indicate that pyroclastics were primarily distributed outside the caldera (Carter et al., 2013). Carter et al. (2013) note that Ina does not have low CPR values relative to the surrounding terrain, which suggests that if any pyroclastics were produced at Ina, they likely formed a very thin layer and may have been intermixed with blocky regolith preventing detection via radar.

2.1.5. Regolith drainage

Sosigenes is located at the intersection of two graben, and Qiao et al. (2016) suggested that it could have formed when regolith drained into the floor of the graben and onto the top of the dike that produced the graben. This could happen if a volatile-rich dike stalls in the shallow subsurface, forms a graben, and then the gas diffuses to the surface leaving a void behind. Subsequent seismic shaking by impacts would then cause drainage of regolith into the void through the highly fractured graben block. The lower units at Sosigenes would thus be areas in which regolith has drained into the subsurface voids. Qiao et al. (2016) argue that the drainage processes could also cause mechanical disturbance of regolith materials resulting in surface smoothing and brightening consistent with their observation of low sub-resolution roughness on the mounds in Sosigenes. A similar seismic drainage process could have occurred at Ina if it is a drained lava lake with a void rich floor (Head and Wilson, 2016). Head and Wilson (2016) prefer this seismic drainage hypothesis, because instead of requiring recent volcanic activity which contradicts lunar thermal evolution models, it involves ancient volcanism and explains the young appearance of the IMPs through more recent seismic modification.

3. Methods

3.1. Diviner

Diviner is a multi-spectral visible and infrared radiometer onboard the Lunar Reconnaissance Orbiter spacecraft (Paige et al., 2010; Vondrak et al., 2010). Remote measurements of surface and subsurface temperatures are made using measured emission in nine spectral bands, from 0.3 to ~400 μm. Brightness temperatures are determined using onboard calibration and pre-flight measurements of radiometric response functions for each channel. Diviner has acquired brightness temperature measurements over the majority of the lunar surface at multiple local times on a spatial scale of ~250 m (Keller et al., 2016; Williams et al., 2016). In addition

to the multi-spectral brightness temperatures, we also use derived rock abundance and regolith temperatures (Bandfield et al., 2011).

3.2. Rock abundance

Rock abundance (RA) is defined as the fractional area within each measurement pixel occupied by rocks. These rocks are detected by Diviner through a spectral slope in brightness temperatures caused by their warmer nighttime temperatures against the background regolith (“anisothermality”). Although rocks over a range of sizes may produce a thermal signature, Bandfield et al. (2011) modeled rocks as horizontally continuous slabs thicker than ~ 1 m. Assuming rock temperatures from this model, Bandfield et al. (2011) solved for the rock abundance and regolith temperature in every pixel. We use their resulting maps, binned at 128 pixels per degree (ppd), with the understanding that the presence of many small rocks may be mistaken for fewer larger rocks or warmer regolith temperatures.

The lunar surface generally has a very low rock abundance with a global average between $\pm 60^\circ$ latitude of 0.004 (0.4% of the surface covered in rocks). Ghent et al. (2014) showed that in regions with elevated rock abundance, such as the ejecta of young craters, the distribution of the rock abundance values of individual pixels is strongly skewed towards higher rock abundances. This departure from a normal distribution causes the mean and median of the rock abundance values to inadequately represent the distribution of values in the sampled area. Ghent et al. (2014) showed that capturing the variation that occurs between different rocky areas requires measuring the population maximum of each area. They did this by measuring the 95th percentile value ($RA_{95/5}$), which is the value that separates the highest 5% of the sampled area’s rock abundance values from the lower 95%. We use this same approach to characterize the distribution of rock abundance values on the IMPs and their surrounding terrain.

3.3. Regolith thickness

Layering of two materials with different thermal inertias can be detected using the shape of nighttime cooling curves (Putzig and Mellon, 2007). When the regolith is thinner than the diurnal thermal skin depth (~ 10 cm on the Moon), the underlying bedrock can be detected by an abrupt decrease in the cooling rate soon after sunset. This is due to the large thermal mass of the rock, which conducts heat downward during the day, and releases it at night (Paige et al., 1994). The thickness of the overlying regolith can be determined by comparing the nighttime surface temperatures to those of a layer of regolith several times thicker than the diurnal thermal skin depth.

3.4. H-parameter

Typically the lunar regolith is thicker than 10 cm (Shkuratov and Bondarenko, 2001), in which case nighttime regolith temperatures provide information about the regolith density and its vertical variation. Following Vasavada et al. (2012), we assume regolith density follows an exponential vertical profile characterized by a single parameter, H :

$$\rho(z) = \rho_d - (\rho_d - \rho_s)e^{-z/H}, \quad (1)$$

where z is the depth, $\rho_d = 1800 \text{ kg m}^{-3}$ is the density at depth, and $\rho_s = 1100 \text{ kg m}^{-3}$ is the density at the surface. We fit the Diviner nighttime regolith temperature measurements (from Bandfield et al., 2011) using modeled regolith temperatures with H as the free parameter assuming the surface layer has a conductivity of $6.6 \times 10^{-4} \text{ W m}^{-1} \text{ K}^{-1}$ and the deep layer has a conductivity of $3.5 \times 10^{-3} \text{ W m}^{-1} \text{ K}^{-1}$. We then produce derived maps of H at

Table 1

Mean, median, and 95th percentile ($RA_{95/5}$) rock abundance values for the four largest IMPs and their surrounding terrain.

	Mean	Median	$RA_{95/5}$
Sosigenes	1.93%	1.64%	3.99%
Surrounding Sosigenes	0.76%	0.48%	2.18%
Ina	0.70%	0.66%	1.27%
Surrounding Ina	0.36%	0.34%	0.56%
Cauchy-5	1.27%	1.21%	1.78%
Surrounding Cauchy-5	0.46%	0.42%	0.75%
Maskelyne	0.82%	0.81%	1.10%
Surrounding Maskelyne	0.42%	0.40%	0.71%

128 ppd. Higher values indicate lower density regolith in the upper ~ 10 cm, whereas lower values indicate higher densities in this layer. Thermal inertia I scales approximately linearly with the bulk density, since thermal conductivity, k , is proportional to density, ρ , (Fountain and West, 1970), and thermal inertia, I , is proportional to $\sqrt{k\rho}$. Therefore, observed H-parameter variations can be interpreted as differences in the thermal inertia of the regolith. A low H-parameter corresponds to a high thermal inertia which could be caused by a lower regolith porosity and/or a higher concentration of rock fragments that are too small to be excluded from the regolith temperature. We expect lower H values are most likely due to the presence of small rock fragments mixed into the regolith, because Apollo found centimeter size range fragments in many soil samples (Carrier et al., 1991). Areas with more of these centimeter scale fragments would have higher nighttime temperatures than areas with fragments that are mostly millimeter scale and smaller.

3.5. Defining IMP boundaries

For each measurement described above, we compare the values on the IMP to the values of the surrounding terrain. We consider a 0.4° by 0.4° region centered on each IMP. We trace the boundaries of the IMPs using LROC NAC images and compare the values within the boundary to those outside of the boundary but within the 0.4° by 0.4° region. In the case of Sosigenes, we exclude the steep slopes from both measurements. Cauchy-5 and Maskelyne are not in topographic depressions, so there is some ambiguity in the boundary between these IMPs and their surrounding terrain. We consider the region where characteristic IMP terrain is most concentrated. In the case of Cauchy-5, small patches of uneven terrain occur with decreasing frequency with distance from the center. We exclude this region from both measurements, because it is unclear if the terrain in between the disperse patches of uneven terrain is comprised of smooth mounds or ordinary regolith.

4. Results

4.1. Rock abundance

The means, medians, and 95th percentile values of the rock abundance distributions all suggest that IMPs are slightly rockier than their surroundings (Fig. 2, Table 1). While they are slightly rockier than their surroundings, the rock abundance distributions of the IMPs are close to a normal distribution and are only slightly skewed towards higher rock abundances. The 95th percentile values are 3.39%, 1.27%, 1.78%, and 1.10% for Sosigenes, Ina, Cauchy-5, and Maskelyne respectively. Sosigenes has a slightly higher rock abundance than the other three IMPs that we measured, which is probably due to mass wasting from the surrounding steep interior walls. Fig. 3 shows a boulder on the edge of the IMP at the bot-

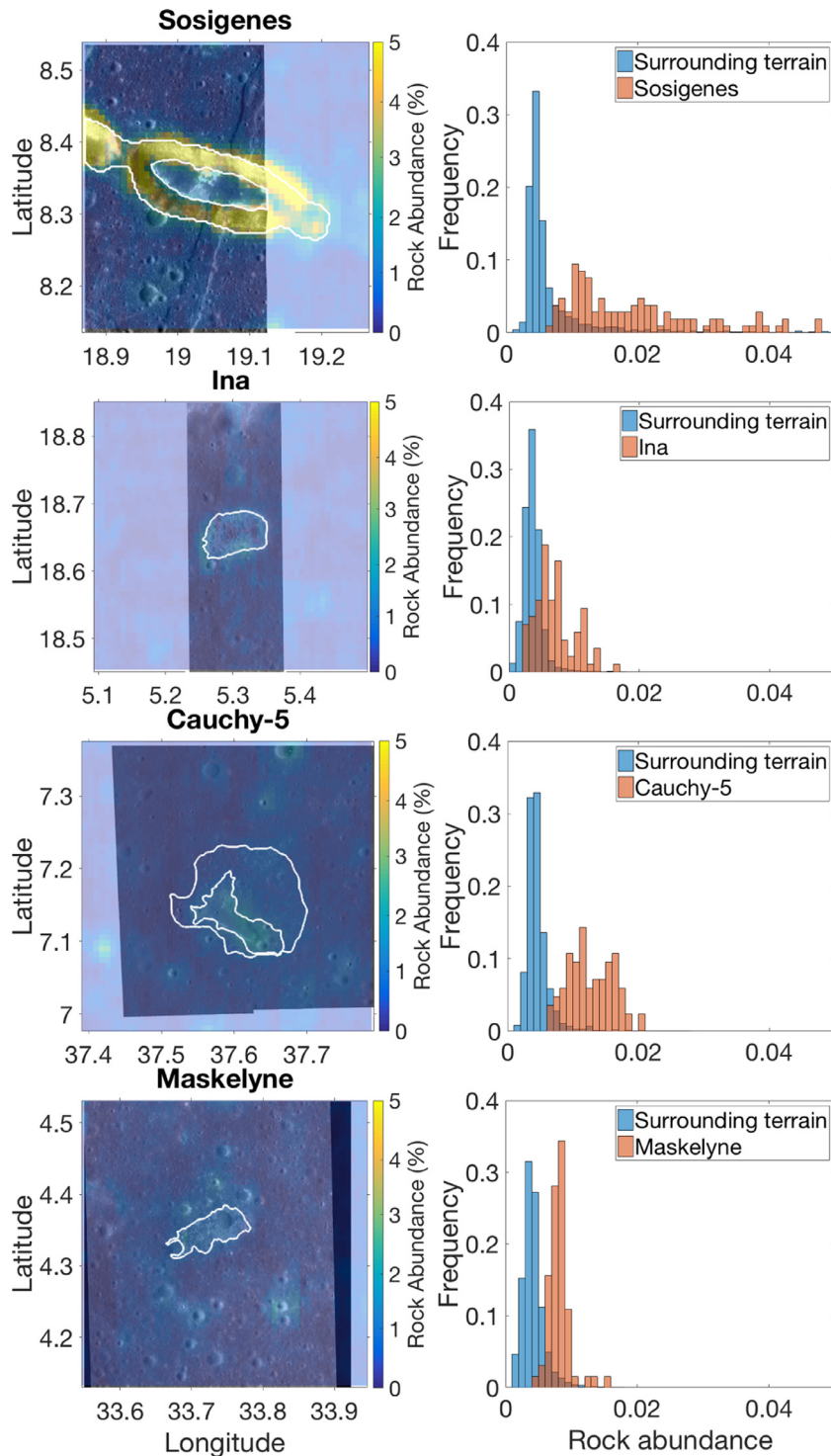


Fig. 2. Rock abundance maps of the four largest IMPs overlain on LROC NAC images (left column): M1129354261 (1.2 m/pix), M119808916 (0.5 m/pix), M1108025067 (1.2 m/pix), and M1129261900 (1 m/pix) respectively; and distribution of rock abundance values (right column) of each IMP (red) and of the terrain surrounding each IMP (blue). White lines indicate the boundary used to separate the IMPs from the surrounding terrain in the histograms. The surrounding terrain histograms include all values outside of the white boundary lines but within the rock abundance maps shown in the left column. Terrain that does not appear to be representative of the IMP or the surrounding terrain (areas between white lines in Sosigenes and Cauchy-5) was excluded from both histograms. (For interpretation of the references to color in this figure legend, the reader is referred to the web version of this article.)

tom of a track which starts part way up a nearby wall. We also note that the rock abundance map of Sosigenes shows that the regions with the lowest rock abundance values are furthest from the slopes (Fig. 4).

4.2. Regolith thickness

Based on thermal model calculations, as described in Hayne and Aharonson (2015), applied to lunar equatorial conditions, we find that a layer of fine grained material less than ~ 15 cm thick overlying rock would be distinguishable from a thicker layer of fine

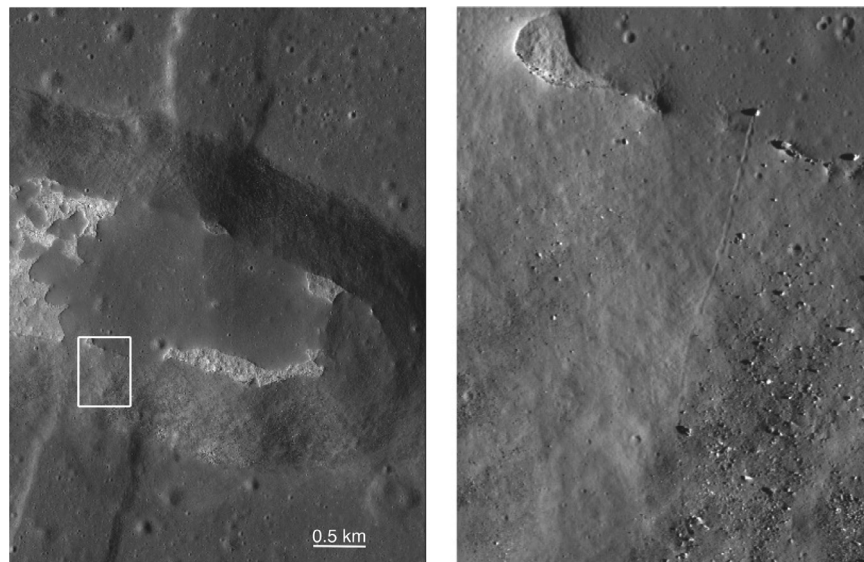


Fig. 3. An example of mass wasting onto the Sosigenes IMP from the surrounding slopes (NAC image M177514916; 0.5 m/pix). The figure on the right shows the area highlighted by the white box in the figure on the left. The boulder at the end of the track is approximately 6 m across.

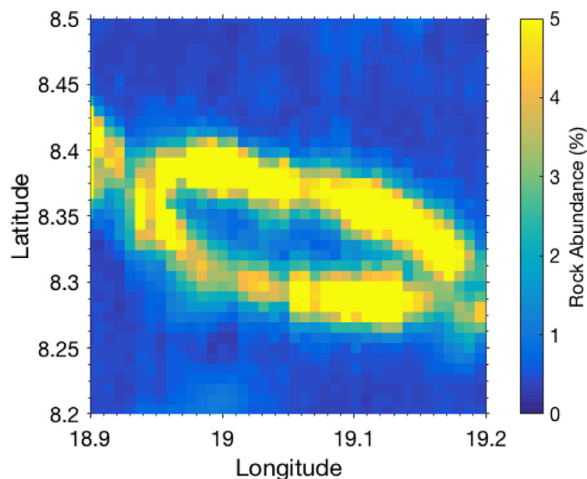


Fig. 4. The rock abundance map of Sosigenes where yellow indicates 5% or more of the surface is covered by rocks and dark blue indicates no rocks. The rock abundance on Sosigenes decreases with increasing distance from the surrounding slopes. (For interpretation of the references to color in this figure legend, the reader is referred to the web version of this article.)

grained material using surface temperature measurements; specifically, the two nighttime cooling curves should diverge (Fig. 5). We consider ten cases ranging from a 2 cm layer of fine grained material overlying rock to a 20 cm layer of fine grained material overlying rock where the regolith has a thermal conductivity of $3 \times 10^{-3} \text{ W m}^{-1} \text{ K}^{-1}$ and a density of 1100 kg m^3 and the rock has the same thermophysical properties as those assumed by Bandfield et al. (2011). The model shows that the surface of a $\sim 15 \text{ cm}$ layer of fine grained material overlying rock and the surface of a layer of fine grained material containing no rock would be indistinguishable with Diviner data. We find that although the IMPs have slightly higher nighttime temperatures (calculated from Diviner channel 7 observations) than their surroundings (expected due to their slightly higher rock abundance), the shapes of the nighttime cooling curves do not differ from that of the surrounding terrain (Fig. 6). In most cases the smooth mounds and uneven terrain are smaller than a single Diviner pixel, so we cannot measure the nighttime cooling curves of each terrain separately. However, if

there is layering in one of these terrains but not the other, it is unlikely that their average nighttime temperature curve would have the same slope as the surrounding regolith. We see no indication of layering, which implies that the layer of regolith or other fine grained material on the four largest IMPs is at least 15 cm thick.

This constraint can be compared to previous model and empirical estimates of regolith formation rates. Arnold (1975) ran Monte Carlo simulations to estimate regolith overturn rates in which they tracked the *disturbed depth* or the thickness of the zone containing material added (due to cratering and/or slumping) during the simulation. They found that the mean disturbed depth scales as $(\text{time})^{0.86}$. In 100 Myr, the Arnold (1975) model would predict overturn of 52 cm of regolith. However, the process of overturning existing regolith differs from the process that would be required if the IMPs started as coherent rock such as would be expected for basaltic lava flows. Rock break down occurs through bombardment by impactors of all sizes ranging from effectively sandblasting to single events capable of disrupting a whole rock (Hörz and Cintala, 1997). Recent work shows that thermal weathering may also play a significant role for certain sized rocks (Molaro et al., 2016; Mazrouei et al., 2016). Hörz et al. (1975) determined rock breakdown rates by conducting Monte Carlo simulations of impacts into rock based on the energy required to break rock and an assumed crater production function. They found that there is a 99% chance that a 10 kg rock (the largest rock they considered) would be destroyed in 68 Myr (Hörz et al., 1975). Basilevsky et al. (2013) and Ghent et al. (2014) both showed that meter scale rocks ($>2 \text{ m}$ and $>1 \text{ m}$ in diameter respectively) in crater ejecta blankets break down faster than the smaller rocks considered by earlier studies such as Hörz et al. (1975). However, breakdown rates of individual rocks may not be representative of the breakdown of a basaltic lava flow either. We also consider the results of Surveyor VII which landed on impact melt covered ejecta from Tycho crater. Tycho has a model age of 85 Myrs (Hiesinger et al., 2012), so it is a reasonable comparison for the IMPs. The Surface Sampler on Surveyor VII encountered rock or a rock below the surface at two locations, but also dug a 15 cm deep trench at another location suggesting that the depth of the regolith layer is irregular ranging from 1 or 2 cm to at least 15 cm (Scott and Roberson, 1968). These results imply that by 100 Myr if the IMPs did contain a layer of coherent rock, it would not be easily detectable by nighttime cooling curves.

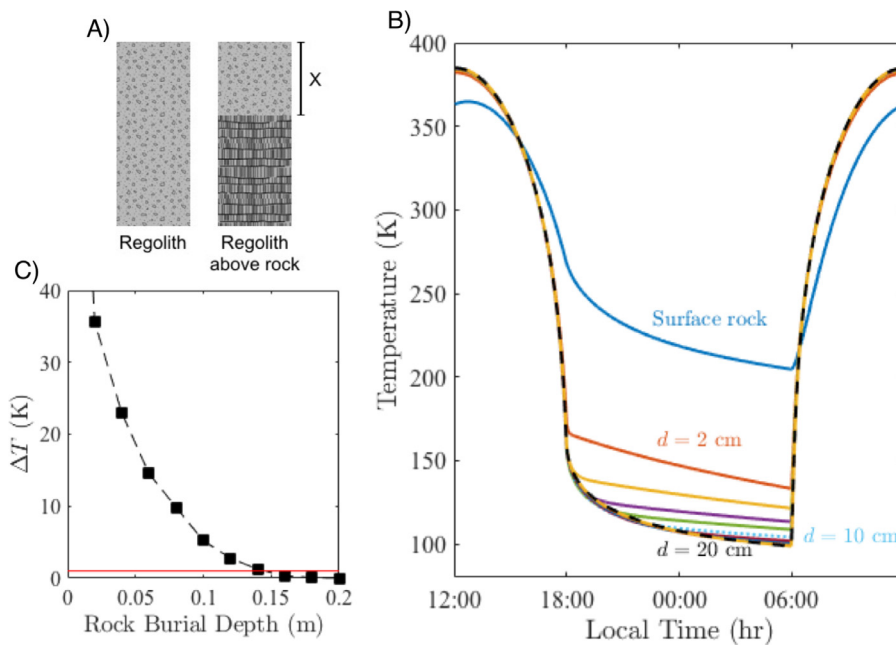


Fig. 5. A) A cartoon depicting the model set up where the left column represents an area where the regolith layer is thicker than the diurnal skin depth and the right column depicts a layer of regolith of thickness X over coherent rock. B) Model surface temperatures during one diurnal cycle. The solid blue line labeled 'surface rock' is the diurnal temperature curve for rock on the surface with no regolith cover. The other curves are diurnal temperature curves for the surface of a regolith layer of thickness X over coherent rock where X increases by increments of 2 cm from 2 cm (solid red line) to 20 cm (dashed black line). C) The difference in temperature at lunar 5 AM of the surface of a layer of regolith over coherent rock and a layer of regolith much thicker than the diurnal skin depth versus the depth of the buried coherent rock. The red horizontal line indicates a 1 K temperature difference; temperature differences smaller than this cannot be detected by Diviner. (For interpretation of the references to color in this figure legend, the reader is referred to the web version of this article.)

Table 2

Mean, median, and 95th percentile ($H_{95/5}$) H-parameter values of the four largest IMPs and their surrounding terrain. A higher H-parameter suggests a lower thermal inertia.

	Mean (m)	Median (m)	$H_{95/5}$ (m)
Sosigenes	0.034	0.035	0.047
Surrounding Sosigenes	0.070	0.072	0.084
Ina	0.090	0.089	0.144
Surrounding Ina	0.078	0.077	0.090
Cauchy-5	0.057	0.056	0.069
Surrounding Cauchy-5	0.071	0.071	0.083
Maskelyne	0.064	0.064	0.070
Surrounding Maskelyne	0.068	0.068	0.081

4.3. H-parameter

We find differences in the H-parameters of the four largest IMPs. H-parameter is the e-folding depth of density increase with depth. Thermal inertia scales approximately linearly with bulk density, so observed H-parameter variations can be interpreted as differences in thermal inertia. The average H-parameter on Ina is 0.090 m, slightly higher than the average H-parameter of its surroundings, 0.078 m (Fig. 7, Table 2). The histogram of H-parameter values on Ina shows a wide distribution that includes values comparable to Ina's surroundings, and values higher than its surroundings (Fig. 7). Closer inspection of the H-parameter map at Ina reveals that although the H-parameter is comparable or slightly higher than the surroundings for much of the IMP, Ina's largest smooth mound has an H-parameter of 0.161 m, significantly higher than Ina's surroundings (Fig. 8). This higher H-parameter suggests a thermal inertia lower than typical regolith. The average H-parameters at Cauchy-5 and Maskelyne are slightly lower than those of the regolith surrounding each IMP (Fig. 7, Table 2), which implies a slightly higher thermal inertia. Sosigenes has an even

lower average H-parameter as compared to its surroundings (Fig. 7, Table 2).

5. Discussion

5.1. Sosigenes

Sosigenes has the highest rock abundance of the four largest IMPs and a higher thermal inertia than the surrounding regolith. In the case of Sosigenes, this elevated thermal inertia is likely due to the presence of small rocks (<1 m) intermixed with the regolith (H-parameter is calculated from the regolith temperatures and therefore excludes the contribution of rocks larger than 1 m). Sosigenes lies at the bottom of a depression surrounded by steep walls, so we expect that mass wasting of rocks of a range of sizes from these slopes (e.g. Fig. 3) elevated the rock abundance and lowered the H-parameter.

5.2. Ina

Ina has an average rock abundance that is slightly higher than the surrounding regolith. The rocky areas are concentrated along the edges of Ina (Fig. 9). A single Diviner pixel is larger than most smooth mounds, but in Ina, pixels that primarily cover a smooth mound generally have a low rock abundance suggesting that the uneven terrain may be the source of the elevated rock abundance which is consistent with previous descriptions of visible imagery (e.g. Braden et al., 2014). Ina has an H-parameter that is higher than the surrounding regolith, which implies the fine grained materials on Ina have a lower thermal inertia than the surrounding fine grained materials. In contrast to the rock abundance, the regions of high H-parameter are concentrated nearer to the center of Ina. A high H-parameter is most easily explained by material containing fewer small rocks (<1 m) than typical regolith or material that is less consolidated than typical regolith. The largest smooth

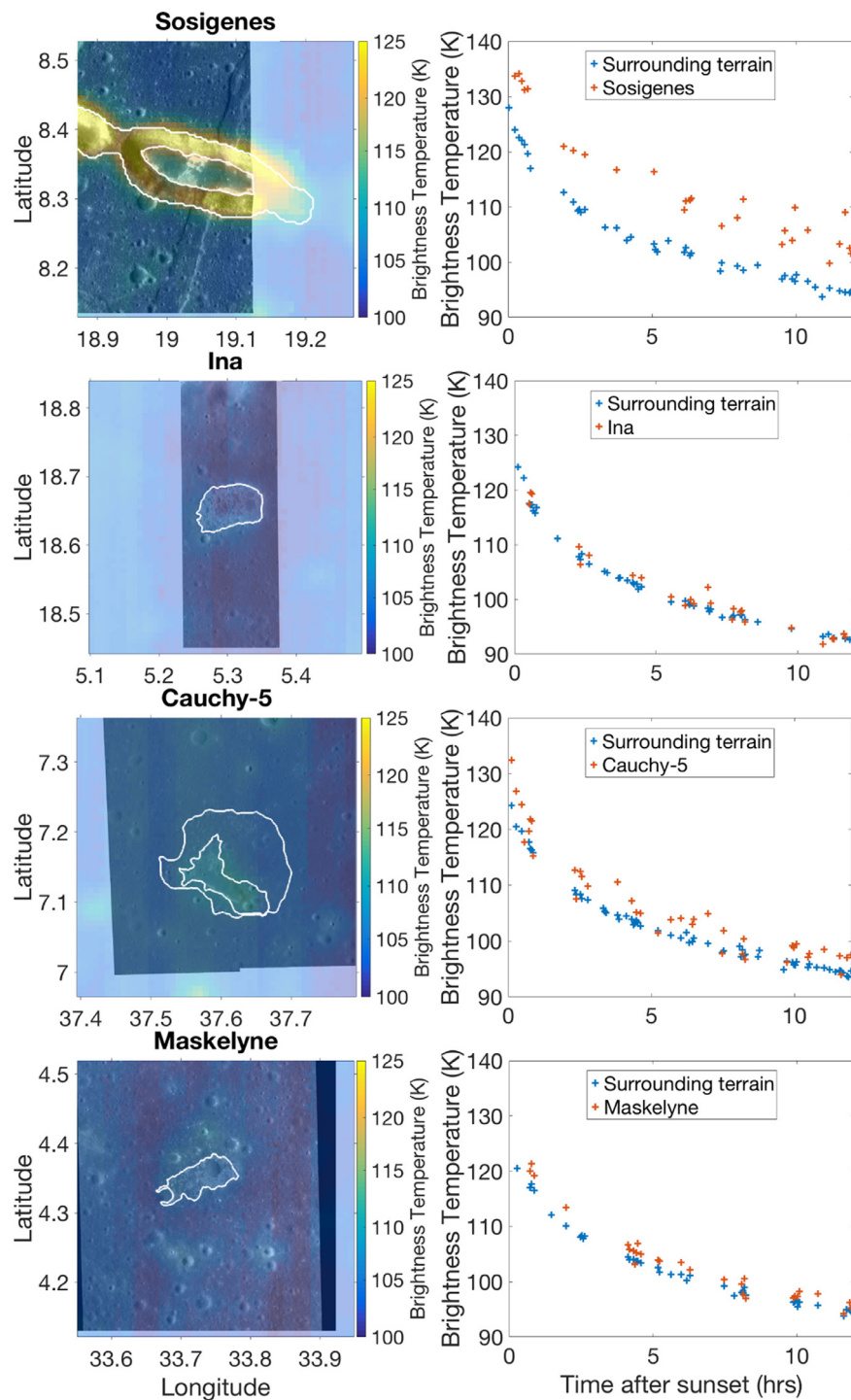


Fig. 6. Maps of the average nighttime brightness temperatures of the four largest IMPs overlain on LROC NAC images (left column): M1129354261 (1.2 m/pix), M119808916 (0.5 m/pix), M1108025067 (1.2 m/pix), and M1129261900 (1 m/pix) respectively; and brightness temperatures of the IMPs (red '+'s) and of the terrain surrounding the IMPs (blue '+'s) versus time after sunset (right column). (For interpretation of the references to color in this figure legend, the reader is referred to the web version of this article.)

mound in Ina exhibits an H-parameter of 0.161 m which is significantly higher than the lunar average of ~ 0.07 m (Fig. 8). The other smooth mounds in Ina are smaller than a single Diviner pixel, so except for the largest mound, pixels in the H-parameter map of Ina represent both the smooth and the uneven terrain. The observation of a low thermal inertia region could be consistent with removal of material from between the mounds and depositing of fine grained material on top of the smooth mounds (either pyroclastic deposits

or deposits of regolith removed by degassing or eruption that are less consolidated than typical regolith after being redeposited). Regions of low thermal inertia in the top few to 10s of centimeters surrounding young craters have been shown to degrade within a few hundred thousand years (Bandfield et al., 2014), so the presence of a region with low thermal inertia at Ina either supports other evidence for a recent formation or implies a thick layer of low thermal inertia material that would take longer to degrade. Al-

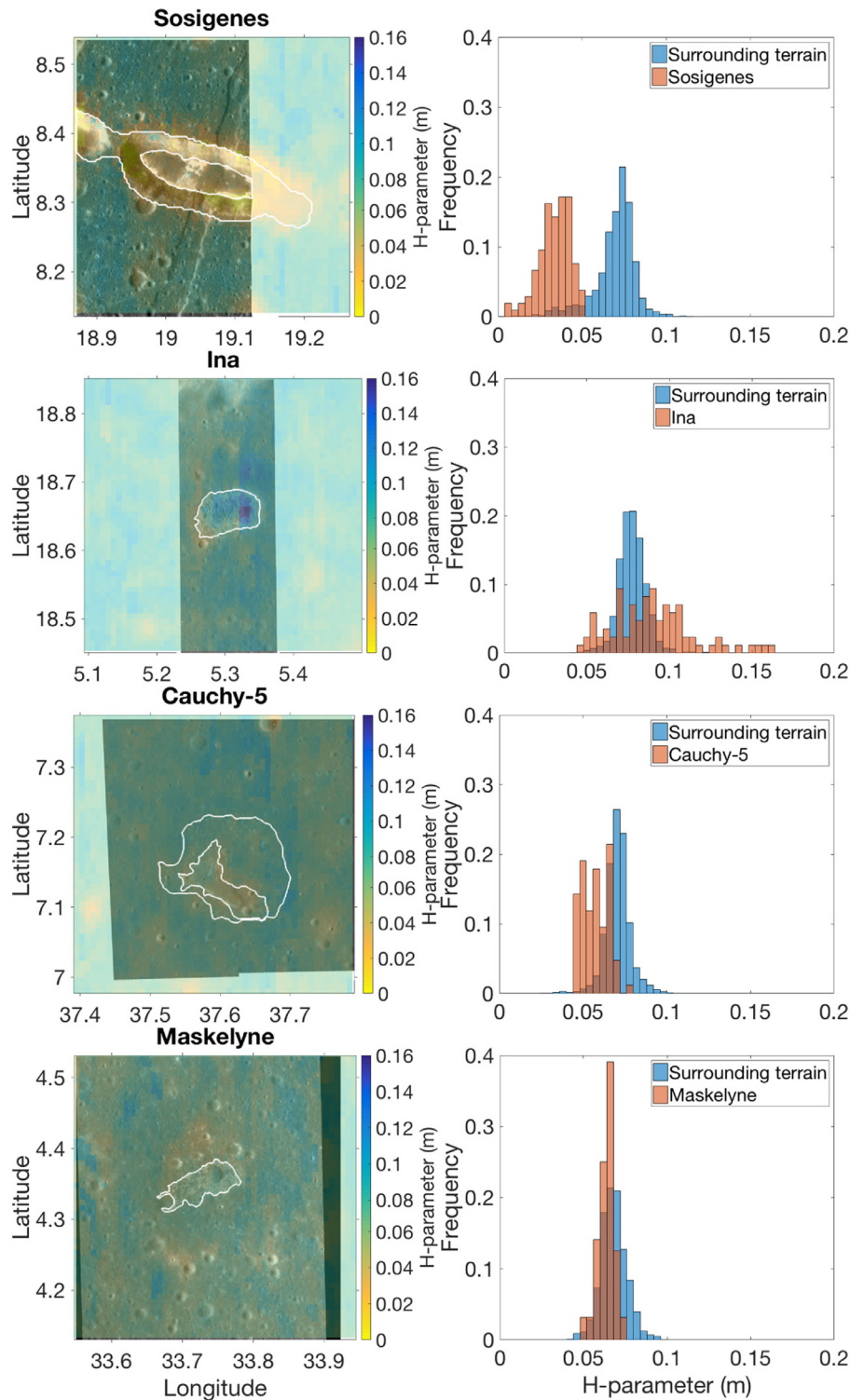


Fig. 7. H-parameter maps (in meters) of the four largest IMPs overlain on LROC images (left column): M1129354261 (1.2 m/pix), M119808916 (0.5 m/pix), M1108025067 (1.2 m/pix), and M1129261900 (1 m/pix) respectively; and distribution of H-parameter values (right column) of each IMP (red) and of the terrain surrounding each IMP (blue). White lines on the maps indicate the boundaries used to separate the IMPs from the surrounding terrain in the histograms. The surrounding terrain histograms include all values outside of the white boundary lines but within the rock abundance maps shown in the left column. Terrain that does not appear to be representative of the IMP or the surrounding terrain (areas between white lines in Sosigenes and Cauchy-5) was excluded from both histograms. Variations in H-parameter are interpreted as variations in thermal inertia (Section 3.4). (For interpretation of the references to color in this figure legend, the reader is referred to the web version of this article.)

though the low thermal inertia region does not preclude the possibility that basaltic lava flows or seismic shaking contributed to the formation of Ina, it is difficult to explain how either of those processes could have resulted in the low thermal inertia material on top of the smooth mound.

5.3. Cauchy-5 and Maskelyne

Cauchy-5 and Maskelyne both have average H-parameters that are slightly lower than the surrounding regolith. However, the H-parameter maps for these two IMPs suggest that the elevated ther-

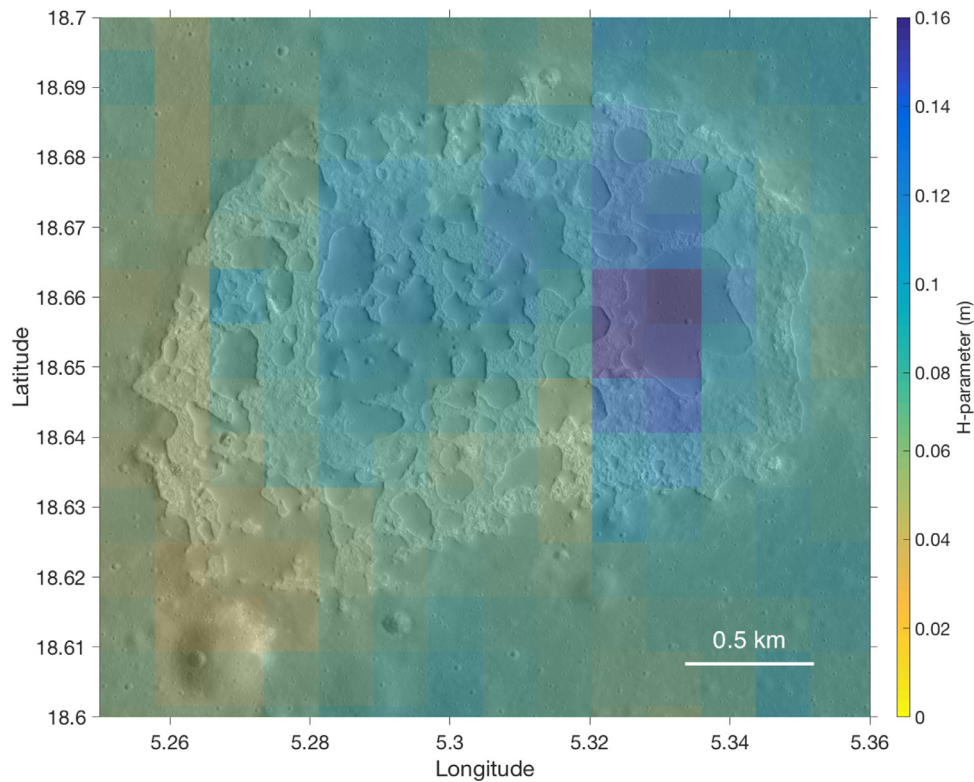


Fig. 8. The H-parameter map for Ina overlain on LROC NAC image: M119808916 (0.5 m/pix).

mal inertia could be due to ejecta from nearby craters (Figs. 1 and 7). This ejecta may also contribute to the slightly elevated rock abundance observed on Cauchy-5 and Maskelyne. LROC images do not reveal large rocks in the ejecta of these craters, but subpixel rocks could also lower the H-parameter and increase the rock abundance. It should be noted that based on LROC NAC DTM's Cauchy-5 and Maskelyne are not confined in depressions as Sosigenes and Ina are, so they do not have distinct boundaries. Rather some small features resembling the uneven terrain appear with decreasing frequency with distance from the center of the IMP. Here we report the average values for the portion of the IMP just where the distinctive features are most concentrated (outlined in white in Figs. 2, 6 and 7).

5.4. Constraining the formation mechanism

In this section we discuss how the results presented in this paper constrain the previously proposed formation hypotheses for the IMPs. We note that it is possible that not all IMPs formed through the same mechanism or that erosion after formation may have altered different IMPs differently. For example, it is possible that all IMPs started with a layer of high H-parameter material that has since been degraded at most IMPs. However, due to the limited number of observational constraints and the high number of proposed formation mechanisms, we test each hypothesized formation mechanism against all available observational data rather than considering each IMP separately. We argue that more data are necessary to fully test the formation hypotheses separately at each IMP. For example, it is possible that all smooth mounds in IMPs have high H-parameters but only Ina has a smooth mound large enough to resolve with Diviner. With these caveats, we assess the previously proposed formation mechanisms in this section and summarize the available constraints and their implications in Table 3.

The first formation mechanism proposed for IMPs, caldera collapse (El-Baz, 1973; Strain and El-Baz, 1980), was based on observations of just Ina. Many of the IMPs discovered more recently are not in topographic depressions at the top of domes (Braden et al., 2014), so this hypothesis is less likely.

Although questions remain about how the Moon could still be out-gassing, removal of materials by sudden degassing can explain most of the available observations. In this scenario, degassing would have removed material from what is now the uneven terrain exposing basaltic surfaces formed 3.5 Gyr ago. This could explain the slightly elevated rock abundance that we observe, because although the smooth mounds should have a rock abundance very similar to the surrounding regolith, the uneven terrain could have a higher rock abundance than mature regolith. Braden et al. (2014) were not able to date the uneven terrain due to the small area, so we can't estimate the thickness of the regolith layer that should have developed since it was first exposed. Although Schultz et al. (2006) state that the removed material formed the faint halo encircling Ina, we suggest that it could have also deposited some material on the mounds within Ina. If this material were less consolidated than mature regolith, it could explain the high H-parameter we measured. Likewise this could explain the smoother sub-resolution surface-textures that Qiao et al. (2016) observed at Sosigenes. If the amount of material removed from the interior and deposited on the surrounding terrain was higher at Cauchy-5, perhaps that could explain the low CPR region observed by Carter et al. (2013). The removal of regolith would also explain the enhanced CPR values Carter et al. (2013) measured in the interior of several IMPs. This hypothesis is also consistent with Qiao et al. (2016)'s observation that at Sosigenes small craters in the uneven terrain have rocks in their crater walls but small craters in the smooth terrain do not. None of the available data directly contradict Schultz et al. (2006)'s hypothesis.

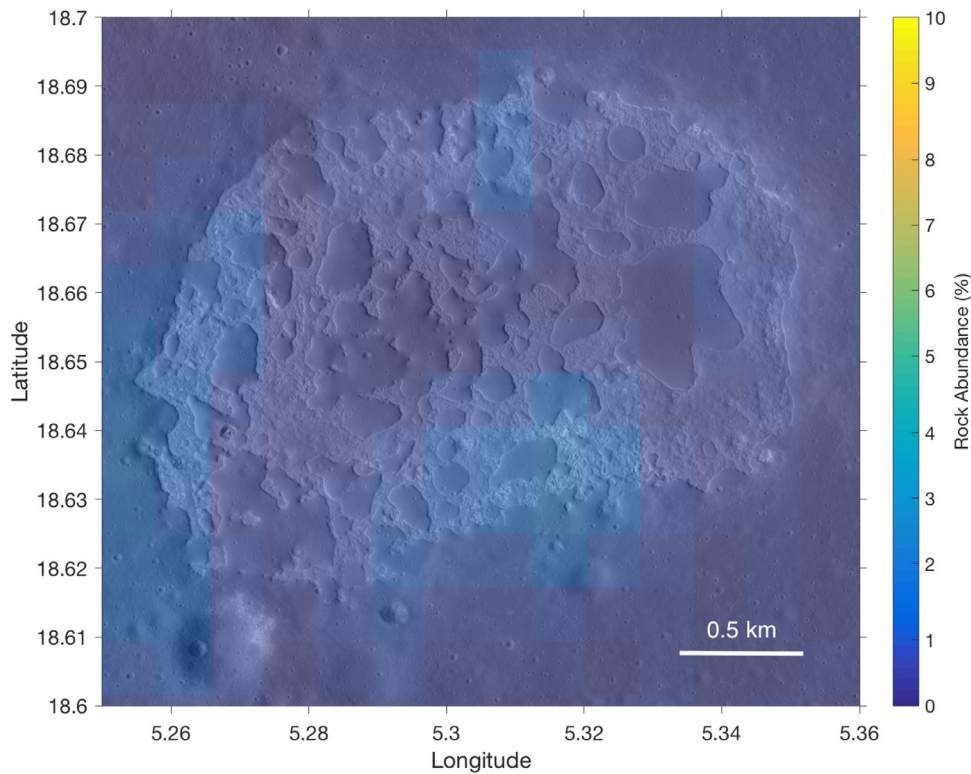


Fig. 9. The rock abundance map for Ina overlain on LROC NAC image: M119808916 (0.5 m/pix).

Garry et al. (2012) argued that Ina was formed by lava flow inflation based on its morphology, but several other data sets contradict this hypothesis. In particular, it is unclear how basaltic lava flows alone could result in a high H-parameter at Ina. If Garry et al. (2012)'s hypothesis that Ina formed through lava flow inflation were extended to other IMPs, it would also inadequately explain the low-CPR halos surrounding Cauchy-5 and Hyginus (Carter et al., 2013) and the meters thick regolith layer implied by crater morphology on the smooth terrain in Sosigenes (Qiao et al., 2016). The observations of slightly elevated rock abundance and a layer of regolith thicker than 15 cm are not strong evidence for or against the lava flow inflation hypothesis. Ghent et al. (2014)'s observation of breakdown of lunar crater ejecta would estimate an $RA_{95/5}$ value of approximately 3% for 100 Myr old ejecta, but it would be reasonable to expect lava flows to have a higher initial rock abundance than crater ejecta and the process of regolith formation could operate differently on different initial surfaces. Regolith overturn models suggest that on average the top 52 cm of regolith would be disturbed in 100 Myr (Arnold, 1975), but the depth of disruption (the thickness of the zone containing material added due to cratering and/or slumping) could differ significantly if the initial surface is coherent rock rather than regolith, so these models may not be appropriate. The basaltic lava flow hypothesis could potentially explain the smoother sub-resolution surface-textures observed at Sosigenes if the early stages of regolith formation involve very small impacts that break apart the coherent rock but do not eject large blocks. Although open questions about the process of regolith formation on a coherent rock surface limit our ability to test the lava flow inflation hypothesis with the rock abundance, regolith thickness, and sub-resolution surface-textures data, the thermal inertia at Ina and the low-CPR regions surrounding Cauchy-5 and Hyginus cannot be explained by lava flows alone.

Carter et al. (2013) suggested that the formation of IMPs may have included pyroclastic eruptions based on low CPR values measured at Cauchy-5 and Hyginus. Pyroclastic eruptions are consis-

tent with other observations of the IMPs using other data sets as well. In particular, if pyroclastic eruptions could remove material in a way similar to the outgassing proposed by Schultz et al. (2006), this hypothesis could explain all observations. As with removal by outgassing, this would predict that the uneven terrain is slightly rockier than the smooth mounds which would cause the elevated rock abundance. The smooth mounds would be coated in pyroclastic deposits which could explain the high H-parameter value on the mound at Ina. If all IMPs formed through pyroclastic eruption, the H-parameter values could vary between the IMPs due to differences in the thicknesses of the deposits or the inclusion or lack of inclusion of country rock. Small craters that formed on mounds covered in a layer of regolith and pyroclastic deposits would not be expected to expose boulders, so this is consistent with Qiao et al. (2016)'s observations of crater morphology at Sosigenes. Pyroclastic deposits would also have a smoother sub-resolution surface texture than regolith (Blewett et al., 2014) consistent with Qiao et al. (2016)'s phase-ratio image results.

Alternatively, instead of removing material from between smooth mounds, pyroclastic eruptions could instead have deposited the smooth mounds. If a pyroclastic fire fountain is optically dense, pyroclasts in the interior of the fountain cannot radiate heat to space because they are shielded by other pyroclasts, so they are still molten when they reach the ground (Wilson and Head, 2016). We suggest that these still molten pyroclasts could contribute to the formation of the unusual morphology of the IMPs by fusing and forming spatter deposits. However, if these were a component of the smooth mounds they would have to be buried by fine grained pyroclasts that solidify before reaching the ground to explain the lack of blocks and the low thermal inertia on the smooth mounds. A scenario such as this could potentially explain the steep margins between the smooth mounds and the uneven terrain.

Qiao et al. (2016) suggested that Sosigenes formed when seismic shaking caused regolith to drain into void space generated

Table 3

Observation predicted for each formation hypothesis for each data set. ✓ means the observations are consistent with the prediction of the hypothesis, X means the observations contradict the prediction of the hypothesis, ✓ ? means that an argument could be made that the observations are consistent with the hypothesis.

	Removal by outgassing		Basaltic lava flows		Pyroclastic eruption		Seismic drainage of regolith	
Rock abundance (this study)	✓	Smooth mounds equivalent to surrounding terrain, uneven terrain is exposed rockier material below.	✓	Initial high rock abundance, now mostly covered in regolith.	✓ ?	Low rock abundance in areas of pyroclastic deposits.	✓	Some regolith remains on most surfaces, but rock may be exposed in areas of drainage (Qiao et al., 2016).
H-parameter (this study)	✓ ?	Material removed could be redeposited with a different porosity than the pre-existing regolith.	X	Equivalent to surrounding terrain.	✓	Could vary based on inclusion or lack of inclusion of country rock in the pyroclastic deposits or thickness of the deposit.	X	Finer regolith grains would preferentially drain leaving behind coarser grains on uneven terrain. Smooth terrain, similar to surrounding terrain.
Radar (Carter et al., 2013)	✓ ?	Rocks are closer to the surface where material has been removed. Removed material might form a low CPR halo.	X	Rocky layer beneath regolith on mounds. No effect on the surrounding terrain.	✓	The pyroclastic deposits would have a low-CPR.	X	Graben block should look rockier in areas where regolith has drained away. No effect on the surrounding terrain.
Crater Morphology (Qiao et al., 2016)	✓	No blocks exposed in small craters on smooth mounds; blocks exposed in craters on uneven terrain.	X	Blocks exposed in crater walls of impacts that puncture deeper than ~50 cm on the smooth mounds.	✓	No blocks exposed in small craters on smooth mounds; blocks exposed in craters on uneven terrain.	✓	No blocks exposed in small craters on smooth mounds; blocks exposed in craters on uneven terrain.
Phase-ratio (Qiao et al., 2016)	✓ ?	Material removed might be deposited with a different porosity than the pre-explosion regolith.	✓	Young regolith may include fewer small rocks if impacts strong enough to eject large blocks have not yet occurred.	✓	Pyroclastic deposits smoother than surrounding regolith.	✓ ?	Qiao et al. (2016) states that seismic shaking would alter the pore structure of regolith on the smooth mounds but does not explain how this could be avoided in the surrounding terrain.

during graben formation. This could explain the observed rock abundance at the four largest IMPs if enough regolith can drain to expose underlying bedrock. According to this hypothesis thick layers of regolith would remain on the smooth mounds, so it could also explain the lack of boulders surrounding small craters on the mounds of Sosigenes. This hypothesis also has the advantage that it does not require recent volcanism which makes it more consistent with lunar thermal evolution models. However, this hypothesis cannot explain several of the observations of IMPs. It cannot explain the low thermal inertia at Ina, and in fact should likely result in higher than average thermal inertia as Head and Wilson (2016) argued that small regolith particles preferentially drain into voids, maintaining roughness. It also cannot explain the low CPR regions surrounding Cauchy-5 and Hyginus. Qiao et al. (2016) found that the smooth mounds in Ina and Sosigenes have smoother sub-resolution surface texture than typical mature regolith. They argue that seismic shaking could alter the porous structure of the regolith on the mounds resulting in surface smoothing. However, they don't explain why this process would affect the regolith on the smooth mounds and not the regolith surrounding Ina and Sosigenes.

5.5. Implications for lunar volcanism

Qiao et al. (2016)'s seismic shaking hypothesis is the only suggested formation mechanism that could explain the IMPs without requiring recent volcanism, but several observations contradict this hypothesis. Therefore if the ages of the IMPs inferred in previous studies (e.g. Schultz et al., 2006; Braden et al., 2014) are correct, then the puzzle of recent lunar volcanism remains. Mantle convection modeling can only maintain a partially molten layer in the Moon's mantle until 2.5 billion years after the formation of the Moon (Ziethe et al., 2009). Ziethe et al. (2009) argue that given the uncertainty in their model (which ignores the PKT) and the error bars in the ages of the youngest mare basalts dated through

crater counting (1.2 Ga + 0.32 Ga/ −0.35 Ga) that the mantle convection models and the inferred ages of mare basalts are in reasonable agreement (Ziethe et al., 2009). However, the partially molten layer would need to persist an additional 1–2 billion years to explain the inferred ages of the IMPs. A viable explanation for this discrepancy that can also explain all observations of the IMPs has not yet emerged.

Although recent volcanism on the Moon is surprising, pyroclastic eruptions were relatively common on the Moon earlier in its history (Head and Wilson, 2016), so this may further support our conclusion that pyroclastic eruptions contributed to the formation of the IMPs. The top of every propagating dike transporting magma through the crust will include a gas filled tip above a zone of gas rich magma, or 'foam' (Wilson and Head, 2003, 2016). When the dike tip reaches the vacuum of the lunar surface, the foam explosively decompresses into gas entraining melt droplets producing pyroclastic beads (Wilson and Head, 2003). Thus all lunar basaltic eruptions should have some component of explosive activity (Wilson and Head, 2016). The details of how an explosive eruption would form the morphology of the IMPs are still uncertain, but based on the halos of block-poor material surrounding Cauchy-5 and Hyginus; the low thermal inertia material on Ina's largest smooth mound; and the prevalence of explosive eruptions on the Moon, it seems likely that the formations of the IMPs included an explosive component.

6. Conclusion

IMPs are slightly rockier than the surrounding regolith, but their rock abundance is low relative to a fresh lava flow. The nighttime cooling curves of the IMPs are slightly higher than the surrounding terrain (due to the higher rock abundance), but the shape of the curves do not differ from that of the surrounding terrain, which suggests that on average there is not a layer of buried rock in the top 15 cm of the IMPs. Low H-parameter measurements

suggest that the average thermal inertias of Sosigenes, Cauchy-5, and Maskelyne are higher than the surrounding terrain. This is most likely due to the presence of small rocks (<1 m) possibly due to ejecta from nearby impacts or in the case of Sosigenes, mass-wasting. By contrast, the average thermal inertia of Ina is lower than that of its surrounding region. In particular, the largest smooth mound in Ina has an especially low thermal inertia. This could be explained by less consolidated regolith or by the presence of fine-grained material including fewer rock fragments than typical regolith. Many formation hypotheses have been suggested to explain IMPs, but removal of material by outgassing or pyroclastic eruptions are the two hypotheses that can best explain the available observations. This does not preclude the possibility that lava flow inflation or seismic shaking contributed to the formation of the IMPs, but it is difficult to understand how these processes could explain the low thermal inertia at Ina, dark halos surrounding several of the IMPs, or a low-CPR region surrounding Cauchy-5.

Acknowledgements

We thank two anonymous reviewers for their helpful suggestions. This work was supported by the NASA Lunar Reconnaissance Orbiter project. The research was carried out at the Jet Propulsion Laboratory, California Institute of Technology, under a contract with the National Aeronautics and Space Administration.

References

- Arnold, J.R., 1975. A Monte Carlo model for the gardening of the lunar regolith. *Moon* 13 (1–3), 159–172.
- Bandfield, J.L., Ghent, R.R., Vasavada, A.R., Paige, D.A., Lawrence, S.J., Robinson, M.S., 2011. Lunar surface rock abundance and regolith fines temperatures derived from LRO Diviner Radiometer data. *J. Geophys. Res.* 116 (E12).
- Bandfield, J.L., Song, E., Hayne, P.O., Brand, B.D., Ghent, R.R., Vasavada, A.R., Paige, D.A., 2014. Lunar cold spots: granular flow features and extensive insulating materials surrounding young craters. *Icarus* 231, 221–231.
- Basilevsky, A., Head, J., Horz, F., 2013. Survival times of meter-sized boulders on the surface of the Moon. *Planet. Space Sci.* 89, 118–126.
- Blewett, D.T., Levy, C.L., Chabot, N.L., Denevi, B.W., Ernst, C.M., Murchie, S.L., 2014. Phase-ratio images of the surface of Mercury: evidence for differences in sub-resolution texture. *Icarus* 242, 142–148.
- Borg, L.E., Shearer, C.K., Asmerom, Y., Papike, J.J., 2004. Prolonged creep magmatism on the Moon indicated by the youngest dated lunar igneous rock. *Nature* 432 (7014), 209–211.
- Braden, S., Stopar, J., Robinson, M.S., Lawrence, S., Van Der Bogert, C., Hiesinger, H., 2014. Evidence for basaltic volcanism on the Moon within the past 100 million years. *Nat. Geosci.* 7 (11), 787–791.
- Carrier, W.D., Olhoeft, G.R., Mendell, W., 1991. Physical properties of the lunar surface. In: *Lunar Sourcebook*, pp. 475–594.
- Carter, L., Hawke, B., Garry, W., Campbell, B., Giguere, T., Bussey, D., 2013. Radar observations of lunar hollow terrain. In: *Lunar and Planetary Science Conference*, 44, p. 2146.
- Carter, L.M., Campbell, B.A., Hawke, B., Campbell, D.B., Nolan, M.C., 2009. Radar remote sensing of pyroclastic deposits in the southern Mare Serenitatis and Mare Vaporum regions of the Moon. *J. Geophys. Res.* 114 (E11).
- Cintala, M. J., McBride, K. M., 1995. Block distributions on the lunar surface: a comparison between measurements obtained from surface and orbital photography. *NASA Technical Memorandum* 104804.
- Donaldson Hanna, K., Evans, R., Bowles, N., Schultz, P., Greenhagen, B., Bennett, K., 2016. Investigating young (< 100 million years) Irregular Mare Patches on the Moon using Diviner observations. In: *Lunar and Planetary Science Conference*, 47, p. 2127.
- El-Baz, F., 1973. D-Caldera new photographs of a unique feature. In: *Apollo 17: Preliminary Science Report*, 330, pp. 30–13–30–17.
- Evans, R., El-Baz, F., 1973. 28. Geological observations from lunar orbit. *Revolution* 1, 28.
- Fernandes, V.A., Burgess, R., Turner, G., 2003. 40ar-39ar chronology of lunar meteorites northwest Africa 032 and 773. *Meteorit. Planet. Sci.* 38 (4), 555–564.
- Fountain, J.A., West, E.A., 1970. Thermal conductivity of particulate basalt as a function of density in simulated lunar and Martian environments. *J. Geophys. Res.* 75 (20), 4063–4069.
- Garry, W., Robinson, M., Zimbelman, J., Bleacher, J., Hawke, B., Crumpler, L., Braden, S., Sato, H., 2012. The origin of Ina: evidence for inflated lava flows on the Moon. *J. Geophys. Res.* 117 (E12).
- Ghent, R.R., Hayne, P.O., Bandfield, J.L., Campbell, B.A., Allen, C.C., Carter, L.M., Paige, D.A., 2014. Constraints on the recent rate of lunar ejecta breakdown and implications for crater ages. *Geology* 42 (12), 1059–1062.
- Grice, J., Donaldson Hanna, K., Bowles, N., Schultz, P., Bennett, K., 2016. Investigating young (< 100 million years) irregular mare patches on the Moon using Moon Mineralogy Mapper observations. In: *Lunar and Planetary Science Conference*, 47, p. 2106.
- Hayne, P.O., Aharonson, O., 2015. Thermal stability of ice on Ceres with rough topography. *J. Geophys. Res.* 120 (9), 1567–1584.
- Head, J.W., Wilson, L., 2016. Generation, ascent and eruption of magma on the Moon: new insights into source depths, magma supply, intrusions and effusive/explosive eruptions (part 2: predicted emplacement processes and observations). *Icarus* 283, 176–223.
- Hiesinger, H., Bogert, C., Pasckert, J., Funcke, L., Giacomini, L., Ostrach, L., Robinson, M., 2012. How old are young lunar craters? *J. Geophys. Res.* 117 (E12).
- Hiesinger, H., Head, J., Wolf, U., Jaumann, R., Neukum, G., 2011. Ages and stratigraphy of lunar mare basalts: a synthesis. *Geol. Soc. America Spec. Pap.* 477, 1–51.
- Hörz, F., Cintala, M., 1997. The Barringer award address presented 1996 July 25, Berlin, Germany: impact experiments related to the evolution of planetary regoliths. *Meteorit. Planet. Sci.* 32 (2), 179–209. doi:10.1111/j.1945-5100.1997.tb01259.x.
- Hörz, F., Schneider, E., Gault, D., Hartung, J., Brownlee, D., 1975. Catastrophic rupture of lunar rocks: a Monte Carlo simulation. *Moon* 13 (1–3), 235–258.
- Kaydash, V., Shkuratov, Y., Korokhin, V., Videen, G., 2011. Photometric anomalies in the Apollo landing sites as seen from the Lunar Reconnaissance Orbiter. *Icarus* 211 (1), 89–96.
- Keller, J., Petro, N., Vondrak, R., et al., 2016. The Lunar Reconnaissance Orbiter mission—six years of science and exploration at the Moon. *Icarus* 273, 2–24.
- Masursky, H., Colton, G.W., El-Baz, F., Doyle, F.J., 1978. Apollo over the Moon: a view from orbit. *NASA Spec. Publ.* 362.
- Mazrouei, S., Ali Lagoa, V., Delbo, M., Ghent, R., Wilkerson, J., 2016. Does thermal fatigue play a role in lunar regolith formation? In: *Lunar and Planetary Science Conference*, 47, p. 1785.
- McKay, D.S., Heiken, G., Basu, A., Blanford, G., Simon, S., Reedy, R., French, B.M., Papike, J., 1991. The lunar regolith. In: *Lunar Sourcebook*, pp. 285–356.
- Molaro, J., Hayne, P., Byrne, S., 2016. Thermally induced stresses in boulders on the Moon: implications for breakdown. In: *Lunar and Planetary Science Conference*, 47, p. 2919.
- Nyquist, L., Bansal, B., Wooden, J., Wiesmann, H., 1977. Sr-isotopic constraints on the petrogenesis of Apollo 12 mare basalts. In: *Lunar and Planetary Science Conference Proceedings*, 8, pp. 1383–1415.
- Paige, D., Foote, M., Greenhagen, B., Schofield, J., Calcutt, S., Vasavada, A., Preston, D., Taylor, F., Allen, C., Snook, K., et al., 2010. The Lunar Reconnaissance Orbiter Diviner Lunar Radiometer experiment. *Space Sci. Rev.* 150 (1–4), 125–160.
- Paige, D.A., Bachman, J.E., Keegan, K.D., 1994. Thermal and albedo mapping of the polar regions of Mars using Viking thermal mapper observations: 1. North polar region. *J. Geophys. Res.* 99 (E12), 25959–25991.
- Papanastassiou, D., DePaolo, D., Wasserburg, G., 1977. Rb-sr and sm-nd chronology and genealogy of mare basalts from the sea of tranquility. In: *Lunar and Planetary Science Conference Proceedings*, 8, pp. 1639–1672.
- Putzig, N.E., Mellon, M.T., 2007. Apparent thermal inertia and the surface heterogeneity of Mars. *Icarus* 191 (1), 68–94.
- Qiao, L., Head, J., Xiao, L., Wilson, L., Dufek, J., 2016. Sosigenes lunar irregular mare patch (IMP): morphology, topography, sub-resolution roughness and implications for origin. In: *Lunar and Planetary Science Conference*, 47, p. 2002.
- Schultz, P., Staid, M., Pieters, C., 2000. Recent lunar activity: evidence and implications. In: *Lunar and Planetary Science Conference*, 31, p. 1919.
- Schultz, P.H., 1976. Moon morphology: interpretations based on Lunar Orbiter photography.
- Schultz, P.H., 1991. The Moon: dead or alive. In: *Mare Volcanism and Basalt Petrogenesis: Astounding Fundamental Concepts*, p. 45.
- Schultz, P.H., Staid, M.L., Pieters, C.M., 2006. Lunar activity from recent gas release. *Nature* 444 (7116), 184–186.
- Scott, R., Roberson, F., 1968. Soil mechanics surface sampler. In: *Surveyor VII: A Preliminary Report*, pp. 121–161.
- Shkuratov, Y.G., Bondarenko, N.V., 2001. Regolith layer thickness mapping of the Moon by radar and optical data. *Icarus* 149 (2), 329–338.
- Solomon, S.C., Head, J.W., 1980. Lunar mascon basins: lava filling, tectonics, and evolution of the lithosphere. *Rev. Geophys.* 18 (1), 107–141.
- Spohn, T., Konrad, W., Breuer, D., Ziethe, R., 2001. The longevity of lunar volcanism: implications of thermal evolution calculations with 2d and 3d mantle convection models. *Icarus* 149 (1), 54–65.
- Staid, M., Isaacson, P., Petro, N., Boardman, J., Pieters, C., Head, J., Sunshine, J., Donaldson Hanna, K., Taylor, L., 2011. The spectral properties of Ina: new observations from the Moon Mineralogy Mapper. In: *Lunar and Planetary Science Conference*, 42, p. 2499.
- Stooke, P., 2012. Lunar meniscus hollows. In: *Lunar and Planetary Science Conference*, 43, p. 1011.
- Strain, P., El-Baz, F., 1980. The geology and morphology of Ina. In: *Lunar and Planetary Science Conference Proceedings*, 11, pp. 2437–2446.
- Taylor, S.R., 1982. *Lunar Science: A Lunar Perspective*, 3303. Citeseer.
- Vasavada, A.R., Bandfield, J.L., Greenhagen, B.T., Hayne, P.O., Siegler, M.A., Williams, J.-P., Paige, D.A., 2012. Lunar equatorial surface temperatures and regolith properties from the Diviner Lunar Radiometer experiment. *J. Geophys. Res.* 117 (E12).
- Vondrak, R., Keller, J., Chin, G., Garvin, J., 2010. Lunar Reconnaissance Orbiter (LRO): observations for lunar exploration and science. *Space Sci. Rev.* 150 (1–4), 7–22.
- Whitaker, E.A., 1972. An unusual mare feature. In: *Apollo 15: Preliminary Science Report*, 289, pp. 25–84–25–85.

- Williams, J.-P., Sefton-Nash, E., Paige, D., 2016. The temperatures of Giordano Bruno crater observed by the Diviner Lunar Radiometer experiment: application of an effective field of view model for a point-based data set. *Icarus* 273, 205–213.
- Wilson, L., Head, J.W., 2003. Deep generation of magmatic gas on the Moon and implications for pyroclastic eruptions. *Geophys. Res. Lett.* 30 (12).
- Wilson, L., Head, J.W., 2016. Generation, ascent and eruption of magma on the Moon: new insights into source depths, magma supply, intrusions and effusive/explosive eruptions (part 1: theory). *Icarus* 283, 146–175.
- Ziethé, R., Seifert, K., Hiesinger, H., 2009. Duration and extent of lunar volcanism: comparison of 3d convection models to mare basalt ages. *Planet. Space Sci.* 57 (7), 784–796.